RSC Advances

ROYAL SOCIETY OF CHEMISTRY

www.rsc.org/advances

RSC Advances

ARTICLE

Clean photoinduced generation of free reactive oxygen species by silica films embedding MPA-CdTe quantum dots

Gustavo C. S. de Souza,[a] David S. M. Ribeiro,[b] S. Sofia M. Rodrigues,[b] Ana Paula S. Paim,[a] André F. Lavorante,[c] Valdinete L. da Silva,[d] João L. M. Santos, *[b] Alberto N. Araújo*[b] and Maria Conceição B. S. M. Montenegro*[b]

CdTe quantum dots capped with mercaptopropionic acid and with 3.5 nm in size were entrapped in sol-gel films prepared with tetramethyl orthosilicate under mineral acidic catalysis in the presence of Triton X-100 as non-ionic surfactant. The follow-up of the sol-gel process was performed in real-time both with the fluorescent crystal-violet as molecular rotor and with quantum dots. Clusters of nanoparticles with 500 nm in size become homogeneously distributed in films, but preserving initial photoluminescence quantum yields (21%), and emission spectrum and with increased excited state lifetime (65±4 ns) and photostability. Films photoactivation inside a multi-pumping flow system enabled reproducible generation of reactive oxygen species determined by chemiluminescence using the alkaline luminol reagent, thus opening future development of clean and environment friendly analytical applications.

Introduction

Quantum dots (QDs) in colloidal solution have been largely exploited as fluorescent reagents for analytical and biological applications.[1,2] The enhanced photostability, quantum efficiency of luminescence and tenability of emission also turn them attractive alternatives to conventional organic fluorophores in contexts ranging from the improvement of optoelectronic and solar cell devices to sensing and (bio)imaging equipment.[3–6] Those properties can be patterned through elemental composition, crystallinity, size and shape, defects and impurities. The QDs combining zinc or cadmium with oxygen, sulfur, selenium or tellurium as II-VI semiconductive compounds are particularly popular due to direct band gap allowance and the numerous available recipes for synthesis. However, several hazardous effects upon humans and environment are particularly cumbersome. Cadmium for instance, has no recognized physiological role in humans yet dermal, pulmonary and gastrointestinal exposure causes serious kidney, bone and pulmonary damages including cancer.[7] Regulatory agencies like Environmental Protection Agency (EPA) and Occupational Safety and Health Administration impose respectively the limits of 5 μg/L to drinking water and 100 ppb to workplace air in order to restrain biohazard.[8] In turn, engineered nanoparticles in monodisperse colloidal sols exhibit peculiar aggregation, adsorptive and reactive behaviours which include increased metal bioavailability and toxicity to biota.[9,10] Thus, usages based on immobilized QDs and recycling of out of use materials are of great interest, being also beneficial to provide cost-effective analytical applications, reduce wastes and to mitigate environmental concern upon discard. Additionally, the same structured material becomes accessible for multiple purposes, including continuous reactive surface, separation unit or as reusable sensor.[11]

Many efforts have been undertaken to incorporate QDs into silica sol-gel matrices while preserving the initial photoluminescence properties.[12–17] Several two-step procedures, *i.e.* separate preparation of nanostructured particles followed by incorporation in the silica bulk medium, are typically used to immobilize QDs in glass films. In this way, luminescent materials with good mechanical characteristics, high transparency, low UV light sensitivity and high thermal stability could be implemented. The alternative in situ preparation of nanocrystals in molten glasses evidenced low versatility entailing the synthesis process, inevitable particle oxidation, volatilization of metal chalcogenides during glass densification and limited ability to obtain core/shell nanostructures.[18] Room temperature procedures were attempted to synthesise II-VI [19,20] and IV-VI QDs [21] during the hydrolysis-condensation of silica alkoxydes in simpler manner but particle size heterogeneity and high-concentration defects were pointed out as main disadvantages. Thus, bottom-up

[a.] Dep. Química Fundamental, Univ. Federal Pernambuco, Av. Jornalista Aníbal Fernandes, s/n - Cidade Universitária, 50740-560 Recife, PE, Brasil.
[b.] LAQV, REQUIMTE, Dep.Química Aplicada, Fac. Farmácia, Univ. Porto, R. Jorge Viterbo Ferreira 228, 4050-313, Porto, Portugal.
[c.] Dep. Química, Univ. Federal Rural de Pernambuco, R. D. Manuel de Medeiros, S/N, Dois Irmãos, 52171-900 Recife, PE, Brasil.
[d.] Dep. Engenharia Química, Univ. Federal Pernambuco, R. Teresa Mélia s/n Cidade Universitária 50740-521 - Recife, PE – Brasil.
† J.L.M Santos, A.N. Araújo and M.C.B. da Silva are the corresponding authors. E-mail: joaolms@ff.up.pt, anaraujo@ff.up.pt and mcbranco@ff.up.pt
Electronic Supplementary Information (ESI) available: [details of any supplementary information available should be included here]. See DOI: 10.1039/x0xx00000x

approaches are used to prepare hydrophobic or hydrophilic quantum dots aiming in a first step at the careful passivation of unsatisfied dangling bonds at nanoparticles surface which could quench radiative exciton recombination. Only thereafter QDs are added to the pre-hydrolysed, water-alcohol-silica alkoxide monomer sol. Afterwards, hydrolysis and condensation proceeds resulting in final gel immobilization, regardless of the morphology intended for the final product. The use of 3-aminopropyltrimetoxysilane (3-APTMS) or tetraethoxysilane (TEOS) monomers or optimized mixtures of both monomers hydrolysed in water-alcohol medium under basic catalysis conditions is often referred. Both monomers and reaction conditions propitiate long gel times (>24h) with the amine group acting as basic catalyst leading to the final xerogel. The use of the more common tetramethyl orthosilicate (TMOS) as starting monomer and the use of a mineral acid catalyst is sometimes referred to justify unsuccessful trials were immediate flocculation of quantum dots with concomitant luminescent loss occurs.[22–24] Nevertheless, Mulvaney´s [25] group has succeeded to incorporate trialkylphosphine capped CdSe quantum dots into xerogels derived from tetramethyl orthosilicate (TMOS) in basic medium using octylamine as catalyst. The catalyst reduced the gel time from hours to minutes scale but only 5-10% of the native photoluminescence quantum yield was observed.[25]

Herein, it is evidenced that CdTe quantum dots capped with mercaptopropionic acid could be easily entrapped in sol-gel films prepared by means of TMOS under mineral acidic catalysis. However, a non-ionic surfactant must be added to the initial sol in order to preserve native photoluminescence properties. The corresponding films provide a clean long-term ability to produce constant amounts of reactive oxygen species (ROS)[26–32] for chemiluminescent analytical applications in simple flow-systems.

Experimental section

Chemicals and Materials

All solutions were prepared with deionized water (18 MΩ cm) and analytical grade reagents. The following chemicals provided by Sigma–Aldrich® were used: absolute ethanol (99.8%), (3-aminopropyl)trimethoxysilane (3-APTMS, 99%), crystal violet (CV, 90%,), cadmium chloride (CdCl2, 99%), luminol, 3-mercaptopropionic acid (MPA, 99%), methanol (99.8%), nitric acid (70%), tellurium powder (200 mesh, 99.8%), tetraethyl orthosilicate (TEOS, 98%), tetramethyl orthosilicate (TMOS, 98%), Triton™ X-100, sodium borohydride (NaBH4, 99%) and sodium hydroxide.

A 1 mol L^{-1} sodium hydroxide stock solution was prepared by dissolving 40.0 g of NaOH in 1000 ml of deionized water.

A luminol stock solution with the concentration of 1.0×10^{-2} mol L^{-1} luminol was prepared by dissolving 177.1 mg of luminol in 100 mL of an equimolar NaOH solution. The stock solution was kept at low temperature and protected from the

light, when not in use. Whenever necessary, working solutions were prepared from this by simple dilution.

Synthesis of CdTe-MPA quantum dots

The molar ratio of $Cd^{2+}:Te^{2-}:MPA$ was fixed at 1:0.05:1.7 and resulting CdTe QDs capped with MPA were synthesized with some modifications in accordance with the method described by Zou et al.[33] The first stage consisted on the complete reduction of 2.99×10^{-4} mol of tellurium with 4.7×10^{-3} mol of NaBH4 in N2 saturated water to produce NaHTe. The resulting solution was then transferred into a second flask containing 6.59×10^{-3} mol of CdCl2 and 1.02×10^{-2} mol of MPA in 120 mL of N2 saturated water. The pH of the solution was adjusted to 11.5 with a 1.0 mol L^{-1} NaOH solution. The aimed size of CdTe QDs was obtained by fixing the refluxing time to 1h. Finally, the nanoparticles in crude solution were precipitated in absolute ethanol and subsequently separated by centrifugation, dried under vacuum and kept in amber flasks.

Procedure to implement SiO2 films with embedded quantum dots

The SiO2 xerogel was prepared by mixing 2 ml of TMOS, 2 ml of Triton™ X-100, 8 ml of methanol and 1 ml of HNO3 (1 mol L^{-1}) into a 50 mL Teflon beaker, then covered with a glass plate and strongly stirred over 10 hours. About 200 mg of MPA capped CdTe QDs were dispersed in 3 mL of an ionic solution Cd^{2+}/MPA with a molar ratio of 1:3,[34] which was previously adjusted at pH 10 using 1 mol L^{-1} of NaOH solution. As initial step to produce silica films with the QDs entrapped both previous sols were mixed and stirred during 10 min.

The spin-coating technique was used to produce thin films over soda lime glass slides. In order to activate the silanol groups at the surface of glass, immersion into a fresh aqueous solution of nitric acid 1:1 (v:v) for 24 hours was proceeded followed by profuse surface rinsing with water, acetone and oven dried at 100 ºC. The coating procedure consisted on the injection of 1 mL of the silica mixture during 1 s on the glass surface spinning at 500 rpm, and further increasing of the spin rate to 2500 rpm for 2 min in order to obtain films with a homogeneous thickness of about 25 μm. Film ageing and drying was performed at room temperature for further 48 hours.

Instrumentation

The separation of the QDs after synthesis was performed by means of a ThermoElectron Jouan BR4I refrigerated centrifuge (Waltham MA, USA). A Laurell WS-650-23B Spin Coater was employed for silica film deposition on the surface of glass slides. A multi-mode microplate reader (Cytation 3, BIO-TEK) was used in the photoluminescence monitoring of the sol-gel process.

A double-beam Jasco V-660 spectrophotometer (Easton, MD, USA) was used for acquisition of absorption spectra of quantum dots dispersed in solution. Fluorolog Tau-3 Lifetime spectrofluorimeter (Horiba Jobin Yvon, NJ, USA) was used to acquire emission spectra and to perform measurements of the

photoluminescence lifetimes by frequency phase modulation using Ludox as a reference standard (τ = 0.00 ns). The measurements of absolute photoluminescence quantum yields were carried out in a Quantaurus QY C11347-11 spectrometer (Hamamatsu) equipped with an integrating sphere to measure all luminous flux.

The morphology and size of the nanoparticles were investigated by High-resolution transmission electron microscopy (HRTEM) using a JEOL JEM 3010 electron microscope (Tokyo, Japan), operated at an acceleration voltage of 300 kV.

The SEM/EDS analysis of silica films with embedded QDs was performed using a High resolution (Schottky) Environmental Scanning Electron Microscope with X-Ray Microanalysis and Electron Backscattered Diffraction analysis: Quanta 400 FEG ESEM / EDAX Genesis X4M.

Fluorescence microscopy was carried out by means of a Tecnai-20 electron microscope (Philips-FEI) system comprising an inverted epifluorescence microscope (Eclipse TE300, Nikon, Tokyo, Japan) equipped with 10X air objectives, a Polychrome II monochromator (TILL Photonics, Martinsried, Germany) and a CCD camera (C6790; Hamamatsu Photonics, Hamamatsu, Japan).

Flow manifold with in-line generation and detection of ROS

The flow manifold was implemented in a configuration aiming the highest efficiency in generation of ROS and to enhance the sensitivity of chemiluminescence detection (Fig. 1).
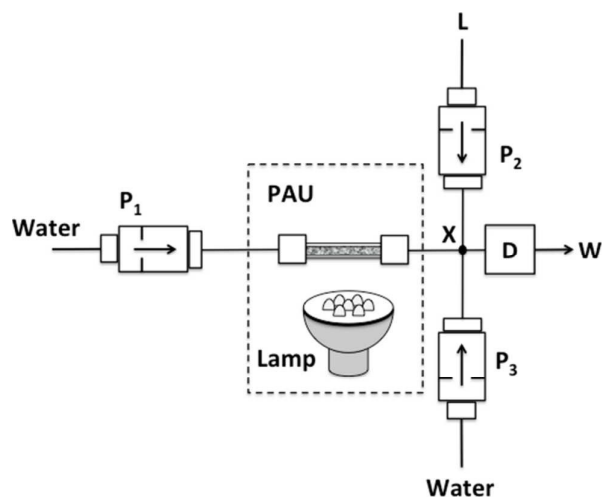

Fig. 1 Schematic representation of the multi-pumping flow manifold. Pi, solenoid micro-pumps; X, confluence point; PAU, photoactivation unit inside a polycarbonate box; D, chemiluminescence detector; L, 0.5 mmol L^{-1} of luminol in 25.0 mmol L^{-1} NaOH solution; LED lamp; W, waste.

It comprised three 120SP solenoid micro-pumps (Bio-Chem Valve Inc. Boonton, NJ, USA) delivering 10 µL per stroke. These

micro-pumps were actuated through a homemade electronic circuit based on the ULN 2803A chip (TOSHIBA) in turn connected to a laptop by means of an USB-6009 interface device (National instruments). The software controlling the micro-pumps and performing data acquisition was developed in LAB VIEW 8.5. The different components of the flow system were connected with 0.8 mm i.d. polytetrafluoroethylene (PTFE) tubing, acrylic homemade end-fittings, and a confluence point. A chemiluminescence detector, model CL-2027 (Jasco, Easton, MD, USA), equipped with a flow cell consisting of a helical 0.8 mm i.d. PTFE tube (100-µL inner volume) placed in front of the photomultiplier tube was used as detection unit. In the outset of the flow manifold special attention was paid to the construction of the photo-activation unit (PAU). It consisted of a small perspex column (40 mm length x 2.5 mm inner diameter) first packed with 100 mg of crushed silica embedding the CdTe QDs and afterwards placed in front to a 6 W LED lamp (Parathorm R50 40 daylight) emitting white light with a luminous flux of 240 lumen. At each end of the column a glass wool stopper was placed to avoid loss of the immobilized material. Because both free radicals and luminescence signal lifetimes is reduced the flow paths between the extremity of the column (placed in PAU), to confluence point X and to entrance of flow-through detection cell were kept as short as possible (about 3 cm).

A 0.4 s time interval for alternate activation of the micro-pumps (1.50 ml min^{-1}, frequency of 2.5 Hz) was initially set in order to fill the tubular with the corresponding solutions, luminol at P_2 and water at P_1 and P_3. The analytical signal baseline was established during activation of P_3. The analytical started with activation of P_1 for 6 sec followed by P_2 for another equal period of time. Finally the detection flow-cell was cleaned and baseline signal reestablished through activation of P_3 during 32 s.

Results and discussion

Characterization of the synthesized CdTe-MPA QDs

The size is one of the most important aspects dictating the unique quantum confinement observed for QDs particles smaller than the exciton Bohr radius.[6] This confinement is characterized by a blue shift in the bandgap energy when the nanoparticle size decreases. In accordance, smaller QDs exhibit photoluminescence in blue region while larger ones emit in the red or even in the near infrared regions. By fixing a particular size of QDs, the observed quantum yields will depend on the minimization of the surface defects that could act as temporary traps for photoinduced charges reducing the experimental quantum yields. In the experimental protocol used careful passivation of the QDs surface assuring adequate solution stability was accomplished with mercaptopropionic acid. Best results were obtained when the molar ratio of Cd^{2+}:Te^{2-}:MPA was fixed at 1:0.05:1.7, enabling the synthesis of red emitting nanoparticles with 22% of quantum yield. The absorption and photoluminescence spectra of the synthesized MPA-capped CdTe QDs are depicted in Fig. 2.
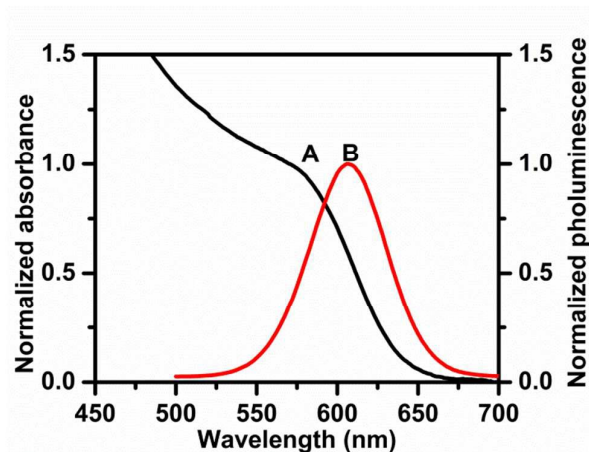
Fig. 2 Normalized UV-Vis absorption (A) and photoluminescence (B) spectra of the synthesized CdTe QDs passivated with mercaptopropionic acid (excitation wavelength 400 nm).
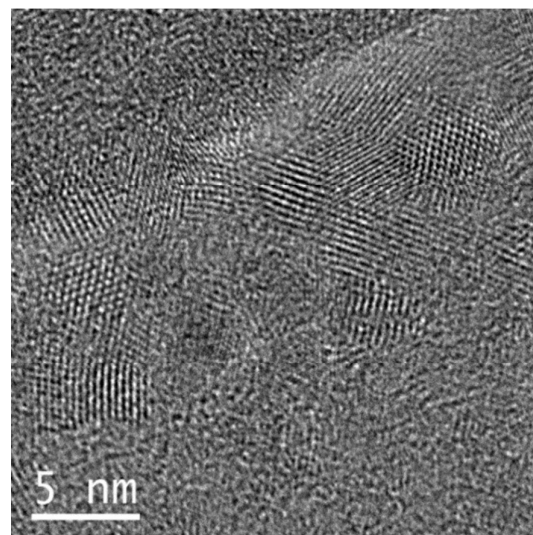

Fig. 3 HRTEM image of the MPA-capped CdTe nanocrystals with lattice planes clearly defined.

It shows a broad absorption band with a maximum for the first excitonic transition located at 587 nm and narrow and symmetric emission band with a maximum intensity at 606 nm, corresponding to an energy bandgap of 2.06 eV. The obtained Full Width at Half Maximum (FWHM) value was of 57 nm, indicating that the synthesized QDs were nearly monodisperse and homogeneous. The average particle size of the QDs was estimated according to the empirical formula proposed by Yu et al.:[35]

$$D = (9.8127 \times 10^{-7})\lambda^3 - (1.7147 \times 10^{-3})\lambda^2 + (1.0064)\lambda - (194.84)$$

with λ(nm) corresponding to the wavelength for the first excitonic absorption peak of the nanoparticle. In accordance, the estimated average particle size was of approximately 3.5 nm. The HRTEM image (Fig. 3) of MPA-CdTe QDs showed monodispersed nanoparticles with nearly spherical shape whose average size is in accordance with the diameter value calculated by the empirical formula proposed by Yu et al.[35] (3.5 nm). Additionally, the existence of lattice planes confirmed the good crystalline structure of the synthesized CdTe QDs.

Thus, the synthesized nanoparticles had adequate properties to allow either the sensitive screening of the immobilization process in silica films and at the same time the evaluation of useful applications.

Entrapment of quantum dots in SiO$_2$ films

The production of silica xerogels by the sol-gel technique has significant advantages such as, the mild chemical conditions used, preparation at room temperature and versatility to tailor the network structure, thickness, the pore size and its distribution.[36]

Table 1 shows the sixteen formulations (F$_1$-F$_{16}$) assayed where the precursor, concentration of catalyst, surfactant volume and water:Si ratio R were varied. In the study, the volumes of methanol co-solvent and of the silica monomer were fixed respectively at 8, and 2 mL. The non-ionic surfactant was used as a stabilizer agent to prevent the QDs surface deterioration and the agglomeration of the colloidal particles during the sol-gel process. The inexistence of specific interactions between the surfactant and QDs was evidenced in previous studies and justified by charge absence in the oxyethylene groups at the polar head.[37,38] On other hand use of a surfactant in formulation of silica films by sol-gel technique reduces shrinkage during ageing and drying processes and fracture occurrence after immersion of the film in water once it lowers surface tension inside pores.[39] Thus, concentration of surfactant stayed in all formulations above the μM range required for the critic micellar concentration. The longer times for gelation observed for tetraethoxysilane (TEOS) and 3-aminopropyltrime-thoxysilane (3-APTMS) formulations relatively to tetramethoxysilane (TMOS) were expected due to their respective slower hydrolysis rates.[40,41] The gelation times also increased with the increase in R, due to greater dilution of hydrolyzed precursors in solution, thus lowering the rate at which condensation process occurs. Xerogels F$_3$, F$_4$, F$_9$, F$_{10}$, F$_{15}$ and F$_{16}$ prepared with higher volume of the alkaline QDs sol had translucent appearance denoting different network structure. While the hydrolysis and condensation process catalyzed at acidic pH leads to a continuously growing network of small condensated oligomers, the raise in pH conditions leads to prompt silica oligomers precipitation. In such conditions the Ostwald ripening process prevails and is responsible for grow of silica particles, which finally aggregate to form an often translucent network.[42]

Table 1 Composition of sols for preparation of films with entrapped CdTe-MPA quantum dots

Films		F_1	F_2	F_3	F_4	F_5	F_6	F_7	F_8	F_9	F_{10}	F_{11}	F_{12}	F_{13}	F_{14}	F_{15}	F_{16}
TMOS	(mL)	2	2	2	2	2	2	-	-	-	-	-	-	-	-	-	-
TEOS	(mL)	-	-	-	-	-	-	2	2	2	2	2	2	-	-	-	-
3-APTMS	(mL)	-	-	-	-	-	-	-	-	-	-	-	-	2	2	2	2
Methanol	(mL)	8	8	8	8	8	8	8	8	8	8	8	8	8	8	8	8
Triton X100	(mL)	2	2	2	2	0.1	0.1	2	2	2	2	0.1	0.1	2	2	0.1	0.1
HNO_3 ($1 mol L^{-1}$)	(mL)	1	-	1	-	1	-	1	-	1	-	1	-	1	-	1	0
HNO_3 ($5 mol L^{-1}$)	(mL)	-	1	-	1	-	1	-	1	-	1	-	1	-	1	-	1
QDs sol	(mL)	4	4	8	8	4	4	4	4	8	8	4	4	4	4	8	8
R ratio Si/water		34	34	67	67	34	34	50	50	100	100	50	50	41	41	81	81
Gelation time	(h)	10	10	>12	>12	10	10	12	12	>15	>15	12	12	>15	>15	<24	<24

In formulations F_5, F_6, F_{11}, F_{12}, F_{15} and F_{16}, the lower volume of Triton X-100 used rendered transparent brittle xerogels, which shrunk significantly in the ageing/drying process. To evaluate the optimum concentration of nitric acid catalyst in the initial precursor mixture, the exchange of QDs sol by a similar volume of a solution containing crystal violet at the concentration of 0.5 g L^{-1} was performed. Crystal violet behaves as non-fluorescent compound in low viscosity medium due to energetic internal conversion enabled by free rotation of dimethylamine functional groups.[43,44] However, with increase in medium viscosity such rotational movements become restrained and fluorescence emerges. Thus, its use was equated in order to provide real time monitoring of microenvironment during gel formation. A steady increase of fluorescence was noticed during the hydrolysis-condensation process whatever the precursor used in the formulations (Fig. 4A).
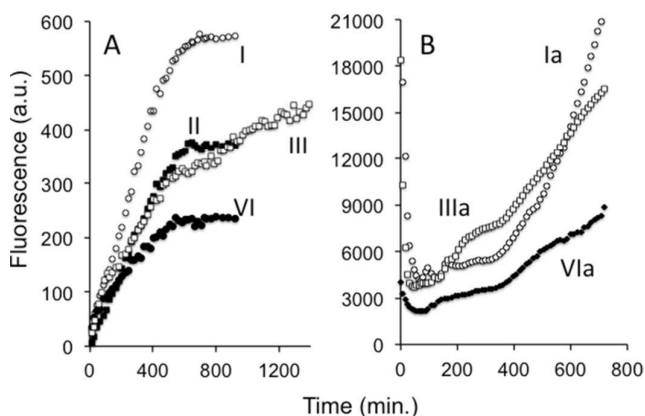

Fig. 4 A) crystal violet fluorescence (λ_{exc}=589 nm, λ_{em}=636 nm) during hydrolysis-condensation of formulations F_1 (I), F_2 (II), F_7 (III) and F_{13} (VI) stated in Table 1. B) Quantum dots fluorescence (λ_{exc}=400 nm, λ_{em}=606 nm) during hydrolysis-condensation of formulations F_1 (Ia), F_7 (IIIa) and F_{13} (VIa).

A relative comparison of microenvironment quality of gels produced with TMOS, TEOS or 3-APTMS is not possible, due to

changes in the molecular rotor behaviour with medium hydrophilic/hydrophobic properties.[45] Nevertheless, gels formed after addition of higher concentrations of nitric acid catalyst (curve II, Fig. 4A) showed much lower intensity of fluorescence relatively to formulations prepared with less concentrated acid. In the former extended segregation of aqueous phase resulted in smaller pores with lower amount of entrapped probe. In contrast, the lower concentration of catalyst enabled better entrapment of the molecular rotor inside the silica network and so the steepest increase of fluorescence (curve I, Fig. 4A). In Fig. 4B, the screening of QDs fluorescence for formulations F_1, F_7 and F_{13} (curves Ia, IIIa and VIa, respectively) is also depicted. In these experiments the quantum dot sols were added in the beginning of the hydrolysis and condensation process, when hydrolysis and condensation reactions leading liberation of alcohols to bulk medium is significant. A drop in fluorescence is observed during the first 90 min after which microenvironment propitiates overpass of the initial values. In accordance to the described by others[22-24], deterioration of particles surface and irreversible loss of photoluminescence was avoided by addition of QDs dispersed in alkaline ionic solution containing cadmium and MPA in the optimized 1:3 proportion. On other hand, the initial fluorescence drop almost vanished when the addition of QDs mixture was performed in later stages of the gelation process, when alcohol evaporation was almost complete and the viscosity of medium was high.

Micrographs performed by scanning electron microscopy (SEM) on aged and dried films obtained with formulations F_1 clearly show uniform spherical aggregates (clusters) of CdTe QDs homogenously dispersed into the silica film (Fig. 5A) with diameters of about 500 nm (Fig. 5B). These aggregates were probably formed during the phase segregation concomitant to network growing and are probably located in pores at the interface between the vesicles of surfactant and the silica phase. Fluorescence microscopy imaging (Fig. 5D) corroborated previous observations since it showed spotted fluorescence emission regularly distributed along the film. A related procedure using surfactant was developed by Murase group which designated it as inverse microemulsion technique and where the protective effect of silica on QDs luminescence was also evidenced.[46]
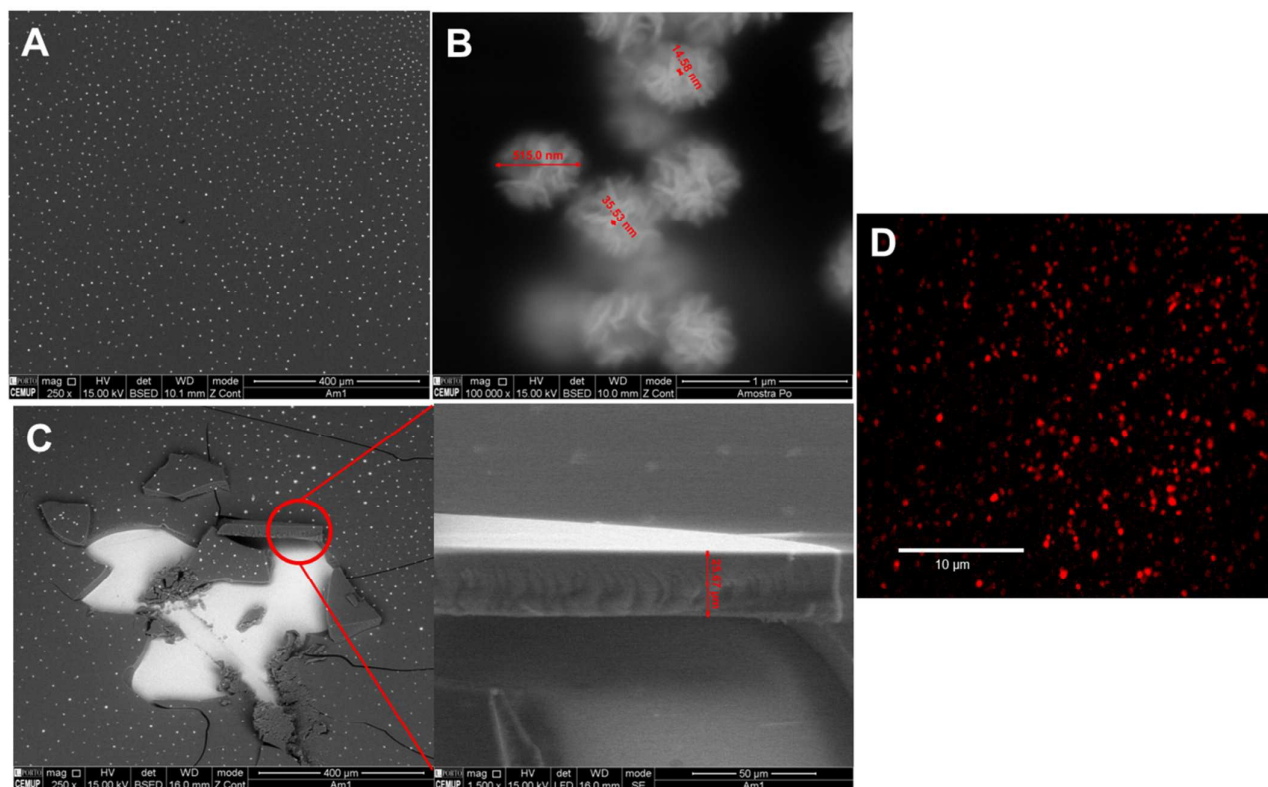
Fig. 5 SEM (A-C) and fluorescence microscopy (D) images of films produced according formulation F_1 where tetratmethyl orthosilicate was used has precursor in the sol-gel process. Micrograph C shows a 25 μm thick uniform film after scratching the surface with a scalpel. In D, intensity of emission decreases according to the deepness of the aggregate in the film.
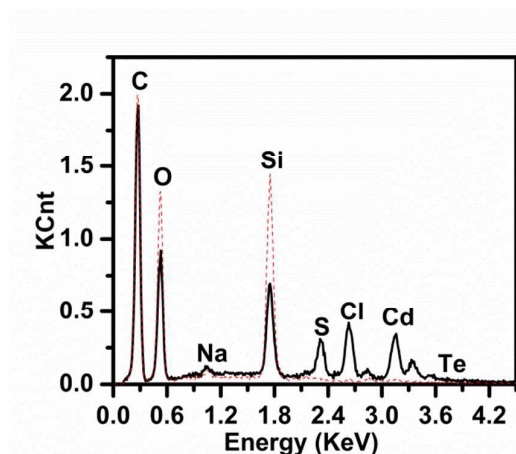

Fig. 6 EDS spectra of the clusters with MPA-CdTe QDs embedded in silica (solid line) and of regions without them (dashed line).

However, the approach has only succeeded to obtain powders using the TEOS as precursor and large volumes of organic solvents.

Additionally, EDS studies were conducted on the film considering both microscope localized clusters of QDs and regions without them. The EDS spectra (Fig. 6) confirmed presence of Cd, Te and S in film regions with QDs only. The Na and Cl peaks observed can be attributed to the precursors used in the MPA – CdTe QDs synthesis (CdCl$_2$ and NaOH).

Comparison between optical properties of the CdTe QDs before and after immobilization

The optical properties of the QDs before and after immobilization in silica films were compared regarding the respective photoluminescence spectra, the photoluminescent lifetimes and quantum yield values. The photoluminescence spectrum of the immobilized QDs obtained after film immersion in a buffer solution at pH 11 is depicted in Fig. 7.

A slightly red shift was observed (Fig. 7B) in the emission peak of the immobilized QDs relatively to QDs dispersed in aqueous solution (from 606 to 611 nm), while no significant differences were observed in the FWHM values. The slight red shift observed can be explained by the vicinity of CdTe QDs in the formed agglomerates and partial energy transfer inside each agglomerate.[47]

In Table 2, the photoluminescence lifetime values of the QDs observed along are shown.

Table 2 Quantum yield and lifetime values of CdTe-MPA QDs with size 3.5 nm before and after the sol-gel process.

	τ (ns)	QY (%)
CdTe-MPA in water	49.69 ± 0.96	22.2 ± 0.2
CdTe-MPA, in Cd^{2+}, MPA solution	22.85 ± 0.68	15.2 ± 0.2
CdTe-MPA QDs in silica film	65 ± 4	21.5 ± 0.4

Firstly, it was observed a decrease of about 54% in photoluminescence lifetime (from 49.69 to 22.85 ns) of nanoparticles in the Cd^{2+}, MPA ionic solution at pH 10 relatively to simple dispersion in water due to adsorption of Cd^{2+} cations on the surface. In authors opinion this adsorption is reversed during the sol-gel process due to both strong Coulomb forces between cadmium cation and free silanol groups and equilibrium shift promoted by the MPA excess in the QDs initial sol used in films formulation. Thus, when the immobilization process ends, the lifetimes increased about 185%, from 22.85 to 65.13 ns (Table 2) due to absence of significant dynamic quenching.[48]
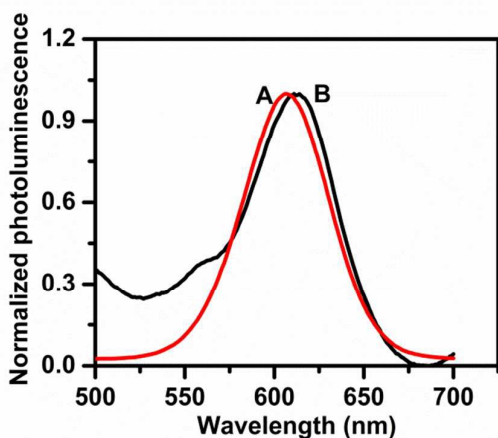

Fig. 7 Normalized photoluminescence spectrum of the CdTe-MPA QDs dispersed in aqueous solution (A) and upon their immobilization in silica (B) (excitation wavelength 400 nm). The shoulder on the left side of B corresponds to background radiation from the soda-lime glass support.

A careful analysis of the quantum yield values also shown that the photoluminescence properties of the QDs dispersed in aqueous solution were not affected by nanoparticles immobilization. In fact, the MPA-CdTe QDs dispersed in aqueous solution showed a quantum yield of 22.2% and 21.5% at the end of the immobilization process. These demonstrate that QDs immobilization by a sol-gel process allows obtaining materials with luminescent properties similar to those observed for QDs dispersed in aqueous solution, with additional advantages arising from a much cleaner and more environmental-friendly utilization in distinct analytical applications.

In order to verify the photoluminescence stability of the films these were assayed during 180 min immersed in a buffer solution pH 11 and profusely rinsed with water between the measurement at intervals of 10 min, setting the excitation and emission wavelengths at 400 and 611 nm, respectively. The results are depicted in Fig. 8 and showed only a slight decrease of the photoluminescence intensity in the first 40 min, followed by constant readings for higher time values.
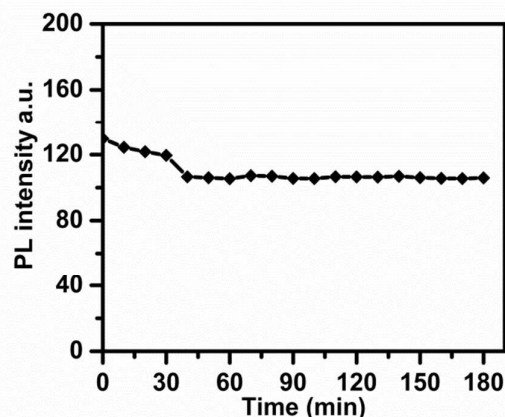

Fig. 8 Photoluminescence intensity (PL) of the immobilized QDs in silica over 180 min (λ_{exc}=400 nm, λ_{em}=606 nm). Irradiation power was of about 180 μW cm^{-2}.

Clean generation of reactive oxygen species

The immobilization of nanoparticles into a solid support can be an expeditious way to assure their continuous re-utilization for analytical purposes, thus avoiding the increased toxicity associated with the single-use aqueous solutions, if their optical properties and reactivity are not impaired. As the photoluminescent properties of QDs in aqueous solution were not altered upon their immobilization in films (similar QY and PL spectra), it was also necessary to demonstrate that the reactivity of the immobilized QDs was unaffected.

The reactivity of the as-prepared films was assessed by using them as continuous multi-use reactors in a flow-based analytical methodology. In these assays, the main aim was to prove, for the first time, that the films preserved the ability to generate reactive oxygen species upon irradiation with visible light as it was already shown for QDs colloidal solutions.[29,31,32] According to these reports, QDs exposed to an electromagnetic radiation with energy equal or higher than the semiconductor bandgap energy promote electron delocalization from the valence band to the conduction band leading to the formation of an exciton (electron–hole pair). The formed excitons possess redox properties, which can trigger chemical reactions with surrounding compounds having redox energies within the crystallite band gap. Some of the above mentioned reports [31,32] indicate the superoxide radical $O_2^{\bullet-}$ as main reactive oxygen species formed since the

conduction band potential of CdTe QDs is sufficient for oxygen reduction (-0.15 eV). In turn, the generated superoxide radical $O_2^{-\bullet}$ can oxidize a chemiluminescent probe and so enable the basis for analytical chemiluminescence. In the present work this reaction scheme was implemented in the multi-pumping flow system represented in Fig. 1, wherein a column packed with 100 mg of crushed films was placed in front of a white LED lamp. Luminol reagent prepared in an alkaline medium was used as luminescence probe (CL) for the ROS detection and only water was made to flow through the packed reactor. Firstly, the influence of luminol concentration on the analytical signal was studied in a range of $0.0125 - 2.5$ mmol L^{-1}, for a constant concentration of NaOH at 10 mmol L^{-1} and halting the flow during the irradiation step for 10 min. This flow time stop was used because preliminary assays indicated that the repeatability and magnitude of luminescence signals were significantly affected without a stopped flow strategy.[49] The obtained results (Fig. 9A) revealed an increase of the analytical signal magnitude with the luminol concentration up to 0.50 mmol L^{-1}.
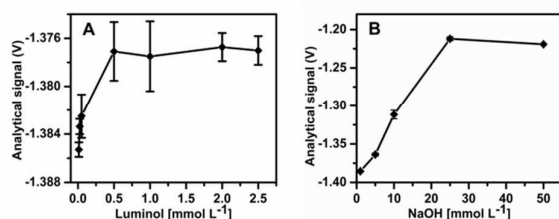

Fig. 9 Influence of the luminol and NaOH concentrations on the analytical signal for a stopped flow of water inside column of 10 min.

Similarly, the influence of the NaOH concentrations on the analytical signal was tested between 1.0 up to 50.0 mmol L^{-1}. For concentration values between 1.0 and 25.0 mmol L^{-1}, a remarkable increase on the analytical signal was observed (Fig. 9B). For higher concentrations no significant differences were observed on the CL intensity. Therefore, the 0.50 mmol L^{-1} luminol solutions were prepared in an alkaline medium with a NaOH concentration of 25 mmol L^{-1}.

As already mentioned, the influence of the irradiation time was important in terms of repeatability and magnitude of the analytical signals. In fact, the response time of silica films used as sensors can be ascribed to the porous structure, the mechanical stability of silica network and the permeability to a given compound.[36,50,51] Therefore, the influence of the irradiation time was studied by exploiting a stopped flow approach,[49] halting the water flow stream in the photoactivation unit (Fig. 1) for 0, 2, 5 and 10 min. Without irradiation no signal was detected since, as expected, the QDs were not photoactivated and excitons were not formed. Then, the obtained results showed an accentuated increase on the CL intensity when increasing the irradiation time between 2 and 5 min. No further signal increase was noticed for 10 min irradiation time.

Once proven the reactivity of the immobilized QDs in silica, it was also important to demonstrate that this new material can be used continuously as a multi-use reactor for the generation of ROS. Therefore, under the optimized conditions, the stability in the generation of ROS was evaluated for 42 consecutive analytical determinations performed during 210 min and repeated in three different days. The obtained results, in Fig. 10, revealed a high repeatability of the signals with a relative standard deviation, RSD, of 1.29 %.
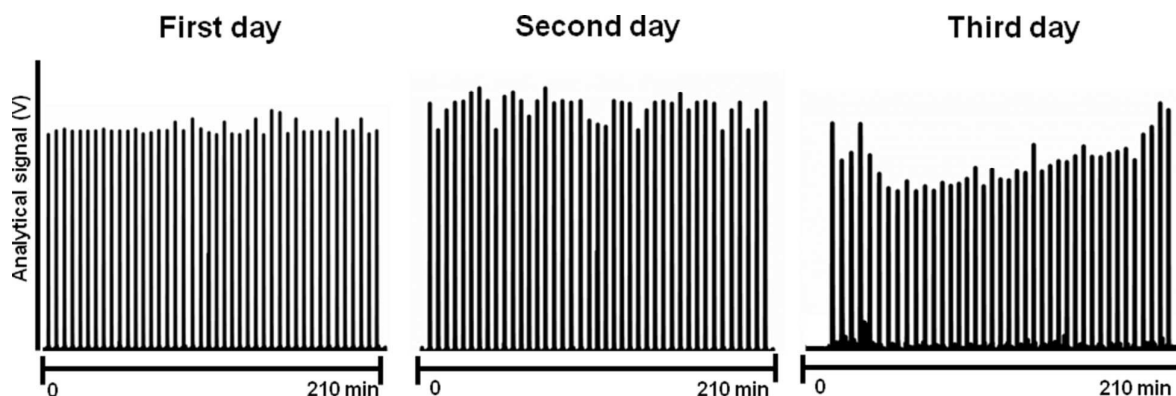

Fig. 10 Signals generated continuously during 210 min and repeated in three different days.

Noteworthy, the generation of hazardous wastes associated with QDs nanoparticles and their core metals, was minimized. In fact, the use of QDs immobilized into a solid support for the generation of ROS allowed a re-utilization of the same reactive surface and consequently no production of hazardous wastes. On contrary, in the scientific works reported in literature that use the QDs dispersed in aqueous solution for the generation of ROS, [29,31,32] a given amount of MPA-CdTe QDs was consumed per determination producing thus hazardous wastes which can be problematic after a long-time use. As example, comparison of proposed methodology with those reported in the literature when consecutive analytical determinations are performed during 210 min, no consumption of CdTe QDs is required, while in the works performed by Ribeiro et al,[29] Sasaki et al [31] and Rodrigues et al.,[32] the amount of QDs consumed during 210 min would be 11300 µg (22 mL of 1.00 µmol L^{-1} MPA-CdTe dispersion), 1036 µg (49 mL of 0.10 µmol L^{-1} GSH-CdTe dispersion), 351 µg (22 mL of 0.15 µmol L^{-1} GSH-CdTe dispersion), respectively.

Conclusions

The production of silica films by the sol-gel process using TMOS, plus Triton X100 respectively as starting monomer and non-ionic surfactant provides effective immobilization of MPA-CdTe QDs rendering materials with the intrinsic properties of starting nanoparticles. Additionally, the sol-gel process via acidic catalysis allowed the production of films with high transparency which is an important factor to emphasize the optical properties of the immobilized nanoparticles and pave the way to chemosensing applications. Herein, the reactivity of the immobilized QDs was also proved through ability to produce reactive oxygen radicals upon visible light irradiation demonstrating also a robust long-term use in chemiluminescent analytical applications. Additionally, the use of the immobilized material for the ROS generation inside an automatic flow system allowed the carrying out of multiple determinations without the production of hazardous wastes in a more environmental friendly approach.

Acknowledgements

Notes and references

1   I. Costas-Mora, V. Romero, I. Lavilla and C. Bendicho, TrAC - Trends Anal. Chem., 2014, **57**, 64–72.
2   Q. Liu, Q. Zhou and G. Jiang, TrAC - Trends Anal. Chem., 2014, **58**, 10–22.
3   Y. Zhu, Z. Li, M. Chen, H. M. Cooper, G. Q. M. Lu and Z. P. Xu, Chem. Mater., 2012, **24**, 421–423.
4   C. Yuanyuan and T. Yifeng, Electrochim. Acta, 2014, **135**, 187–191.
5   H.-Y. Park, I. Ryu, J. Kim, S. Jeong, S. Yim and S.-Y. Jang, J. Phys. Chem. C, 2014, **118**, 17374–17382.
6   D. Bera, L. Qian, T. K. Tseng and P. H. Holloway, Materials (Basel)., 2010, **3**, 2260–2345.
7   J. Godt, F. Scheidig, C. Grosse-Siestrup, V. Esche, P. Brandenburg, A. Reich and D. A. Groneberg, J. Occup. Med. Toxicol., 2006, **1**, 1-6.
8   ASDTR (Agency for Toxic Substances and Disease Registry), Division of Toxicology and Environmental Medicine/Applied Toxicology Branch, Toxicological Profile for cadmium, 2012, U.S. Department of Health and Human Services; Atlanta, Georgia.
9   Y. Yang, J. M. Mathieu, S. Chattopadhyay, J. T. Miller, T. Wu, T. Shibata, W. Guo and P. J. J. Alvarez, ACS Nano, 2012, **6**, 6091–6098.
10 Y. Yang, J. Wang, H. Zhu, V. L. Colvin and P. J. Alvarez, Environ. Sci. Technol., 2012, **46**, 3433–3441.
11 S. S. M. Rodrigues, D. S. M. Ribeiro, C. Frigerio, S. P. F. Costa, J. A. V. Prior, P. C. A. G. Pinto, J. L. M. Santos, M. L. M. F. S. Saraiva and M. L. C. Passos, ChemPhysChem, 2015, **6**, 1880–1888.
12 C. Bullen, P. Mulvaney, C. Sada, M. Ferrari, A. Chiasera and A. Martucci, J. Mater. Chem., 2004, **14**, 1112-1116.
13 M. Ando, C. Li, P. Yang and N. Murase, J. Biomed. Biotechnol., 2007, **2007**, 1-6.
14 Z. Yang and G. Zhou, Adv. Mater. Lett., 2012, **3**, 2–7.
15 R. Koole, M. M. Van Schooneveld, J. Hilhorst, C. M. De Donegá, D. C. 'T Hart, A. Van Blaaderen, D. Vanmaekelbergh and A. Meijerink, Chem. Mater., 2008, **20**, 2503–2512.
16 M.-R. Chao, C.-W. Hu and J.-L. Chen, Biosens. Bioelectron., 2014, **61**, 471–477.
17 T.-W. Sung, Y.-L. Lo and I.-L. Chang, Sens. Actuators, B, 2014, **202**, 1349–1356.
18 D. L. Ou, A. B. Seddon, Phys. Chem. Glas., 1998, **39**, 154–166.
19 L. Spanhel, M. Haase, H. Weller and A. Henglein, J. Am. Chem. Soc., 1987, **109**, 5649–5655.
20 D. Bera, L. Qian, S. Sabui, S. Santra and P. H. Holloway, Opt. Mater. (Amst)., 2008, **30**, 1233–1239.
21 A. Sashchiuk, E. Lifshitz, R. Reisfeld, T. Saraidarov, M. Zelner and A. Willenz, J. Sol-Gel Sci. Technol., 2002, **24**, 31–38.
22 P. Yang, C. L. Li and N. Murase, Langmuir, 2005, **21**, 8913–8917.
23 N. Murase and M. Gao, Mater. Lett., 2004, **58**, 3898–3902.
24 C. Li and N. Murase, Langmuir, 2004, **20**, 1–4.
25 S. T. Selvan, C. Bullen, M. Ashokkumar, P. Mulvaney, Adv. Mater., 2001, **13**, 985–988.
26 B. I. Ipe, M. Lehnig and C. M. Niemeyer, Small, 2005, **1**, 706–709.
27 E. Yaghini, K. F. Pirker, C. W. M. Kay, A. M. Seifalian and A. J. MacRobert, Small, 2014, **10**, 5106-5115.
28 C. I. C. Silvestre, C. Frigerio, J. L. M. Santos and J. L. F. C. Lima, Anal. Chim. Acta, 2011, **699**, 193-197.
29 D. S. M. Ribeiro, C. Frigerio, J. L. M. Santos and J. A. V Prior, Anal. Chim. Acta, 2012, **735**, 69–75.

30 B. Hemmateenejad, M. Shamsipur, T. Khosousi, M. Shanehsaz and O. Firuzi, Analyst, 2012, **137**, 4029.

31 M. K. Sasaki, D. S. M. Ribeiro, C. Frigerio, J. A. V Prior, J. L. M. Santos and E. A. G. Zagatto, Luminescence, 2014, **29**, 901–907.

32 D. M. C. Rodrigues, D. S. M. Ribeiro, C. Frigerio, S. S. M. Rodrigues, J. L. M. Santos and J. A. V. Prior, Talanta, 2015, **141**, 220–229.

33 L. Zou, Z. Gu, N. Zhang, Y. Zhang, Z. Fang, W. Zhu and X. Zhong, J. Mater. Chem., 2008, **18**, 2807–2815.

34 P. Yang and N. Murase, Adv. Funct. Mater., 2010, **20**, 1258–1265.

35 W. Yu, L. Qu, W. Guo and X. Peng, Chem. Mater., 2003, **15**, 2854–2860.

36 P. C. A. Jerónimo, A. N. Araújo and M. Conceição B S M Montenegro, Talanta, 2007, **72**, 13–27.

37 M. Hamity, R. H. Lema and C. A. Suchetti, J. Photochem. Photobiol., A, 2000, **133**, 205–211.

38 M. Lavkush Bhaisare, S. Pandey, M. Shahnawaz Khan, A. Talib and H.-F. Wu, Talanta, 2015, **132**, 572–578.

39 C. Rottman, M. Ottolenghi, R. Zusman, O. Lev, M. Smith, G. Gong, M. L. Kagan and D. Avnir, Mater. Lett., 1992, **13**, 293–298.

40 A. Vainrub, F. Devreux, J. P. Boilot, F. Chaput and M. Sarkar, Mater. Sci. Eng. B, 1996, **37**, 197–200.

41 K. Yoshikawa, S. Nakata, T. Omochi and G. Colacicco, Langmuir, 1986, **2**, 715–717.

42 C. J. Brinker and G. W. Scherer, Sol-Gel Science: The Physics and Chemistry of Sol-Gel Processing, Academic Press, San Diego, CA, 1990.

43 B. Valeur and M. N. Berberan-Santos, Molecular Fluorescence: Principles and Applications, Wiley, Weinheim, Germany, 2nd ed., 2012.

44 R. O. Loutfy, Pure Appl. Chem., 1986, **58**, 1239–1248.

45 M. A. Haidekker, T. P. Brady, D. Lichlyter and E. A. Theodorakis, J. Am. Chem. Soc., 2006, **128**, 398–399.

46 S. T. Selvan, C. Li, M. Ando and N. Murase, Chem. Lett., 2004, **33**, 434–435.

47 C. L. Li, M. Ando and N. Murase, J. Non-Cryst. Solids, 2004, **342**, 32–38.

48 H. D. Duong, C. V. G. Reddy, J. I. Rhee and T. Vo-Dinh, Sens. Actuators, B, 2011, **157**, 139–145.

49 J. Růžička and E. H. Hansen, Anal. Chim. Acta, 1979, **106**, 207–224.

50 W. S. Han, H. Y. Lee, S. H. Jung, S. J. Lee and J. H. Jung, Chem. Soc. Rev., 2009, **38**, 1904–1915.

51 C. Triantafillidis, M. S. Elsaesser and N. Hüsing, Chem. Soc. Rev., 2013, **42**, 3833–3846.

CdTe-MPA QDs immobilized into silica films with highly transparency were obtained by sol-gel technique by using TMOS. Immobilized nanomaterials preserved their native photoluminescence and also their ability to generate ROS opening perspectives for the development of more environment friendly analytical application.